

# Beads-on-a-String Structure of Long Telomeric DNAs under Molecular Crowding Conditions

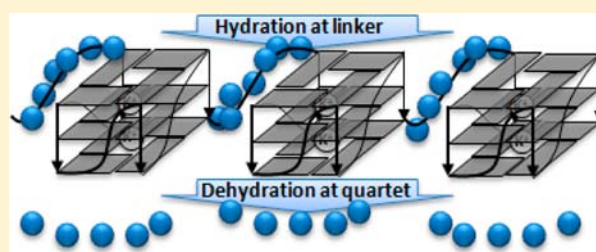
Haiqing Yu,<sup>†</sup> Xiaobo Gu,<sup>†</sup> Shu-ichi Nakano,<sup>†,‡</sup> Daisuke Miyoshi,<sup>\*,†,‡</sup> and Naoki Sugimoto<sup>\*,†,‡</sup>

<sup>†</sup>FIBER (Frontier Institute for Biomolecular Engineering Research), Konan University, 7-1-20 Minatijima-Minatomachi, Chuo-ku, Kobe 650-0047, Japan

<sup>‡</sup>FIRST (Faculty of Frontiers of Innovative Research in Science and Technology), Konan University, 7-1-20 Minatijima-Minatomachi, Chuo-ku, Kobe 650-0047, Japan

**S** Supporting Information

**ABSTRACT:** The structure and stability of long telomeric DNAs,  $(T_2AG_3)_n$  ( $n = 4-20$ ), were studied under dilute and molecular crowding conditions in the presence of  $Na^+$  and  $K^+$ . Structural analysis showed that the long telomeric DNAs formed intramolecular G-quadruplexes under all conditions. In the presence of  $Na^+$ , the telomeric DNAs formed an antiparallel G-quadruplex under both dilute and molecular crowding conditions. However, in the presence of  $K^+$ , molecular crowding induced a conformational change from mixed to parallel. These results are consistent with numerous structural studies for G-quadruplex units under molecular crowding conditions. Thermodynamic analysis showed that G-quadruplexes under the molecular crowding conditions were obviously more stable than under dilute condition. Interestingly, this stabilization effect of molecular crowding was reduced for the longer telomeric DNAs, indicating that the G-quadruplex structure of long telomeric DNAs is not as stable under molecular crowding conditions, as implied from the large stabilization of isolated G-quadruplex units as previously reported. Moreover, a hydration study revealed that upon structure folding, the interior of a G-quadruplex unit was dehydrated, whereas the linker between two units was more hydrated. It is thus possible to propose that the linkers between G-quadruplex units are ordered structures but not random coils, which could have an important influence on the stability of the entire structure of long telomeric DNAs. These results are significant to elucidate the biological characteristics of telomeres, and can aid in the rational design of ligands and drugs targeting the telomere and related proteins.



## INTRODUCTION

The termini of eukaryotic chromosomes contain structures known as telomeres, which are composed of tandemly repeated guanine-rich (G-rich) and complementary cytosine-rich (C-rich) noncoding sequences.<sup>1</sup> In most organisms, the G-rich strand extends beyond the G-rich/C-rich region of the telomere as a single-stranded 3'-overhang.<sup>2-4</sup> The G-rich strand can form G-quartets containing four coplanar guanines stabilized by Hoogsteen-type hydrogen bonds and by the coordination of specific metal ions, such as  $Na^+$  and  $K^+$ , to O6 of guanine<sup>5-10</sup> (Figure 1A). An array of G-quartets stacking with each other results in a highly stable structure called a G-quadruplex (Figure 1B), which protects chromosomes from being recognized as DNA strand breaks and from end-fusing and fraying.<sup>11</sup> Moreover, the formation of G-quadruplexes of the G-rich strand in the 3'-overhang can maintain the length of telomeres by repelling telomerase, which adds the repeating G-rich sequence to the 3' end of chromosomes.

In human somatic cells, the telomeric DNA is typically 5–8 kb in length, and most of the telomeric DNA may form a duplex between the G-rich and C-rich sequences. However, the length of the G-rich 3'-overhang in human somatic cells is usually  $200 \pm 75$  bases.<sup>12</sup> Recently, the telomeric repeat-

containing RNA (TERRA) was found in mammalian cells.<sup>13,14</sup> TERRA has gained increasing attention since it was first proposed to be important in cellular differentiation and development.<sup>15</sup> Interestingly, TERRA is more abundant when telomeres are long,<sup>13,14</sup> indicating the importance of telomere length not only in telomerase function but also in a broad spectrum of cellular events. To date, most studies however have focused on G-quadruplex units composing 20–30 bases, and only a limited number of reports have focused on longer telomeric sequences.<sup>16-29</sup> Therefore, it is still unclear whether long telomeric DNA has the same characteristics as short G-quadruplex units, or has distinct features that cannot be deduced from the G-quadruplex unit. This is partly due to the polymorphic nature of G-quadruplex structure and stability, which critically depends on the combination of nucleotide sequence and surrounding environmental factors involving cationic species, their concentrations, and molecular crowding.<sup>20,21,30-34</sup> Thus, further studies on long telomeric G-rich strands, as well as the short ones in cell-like conditions, are

Received: June 4, 2012

Published: August 30, 2012

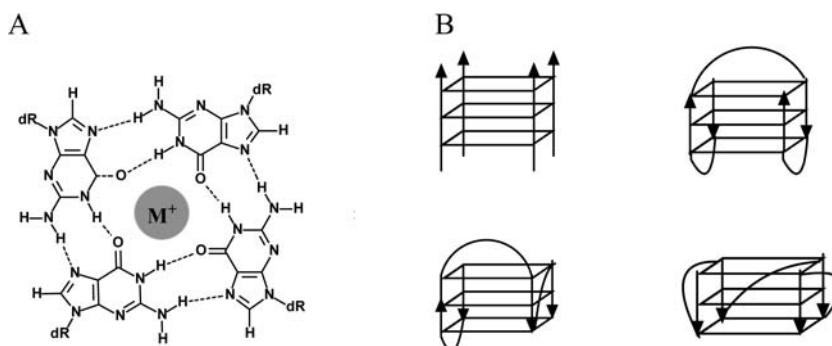


**Figure 1.** (A) Chemical structure of a G-quartet. (B) Schematic illustration of the various G-quadruplexes.

required for understanding biological processes and diseases related to the telomere.

Most biochemical and biophysical studies of G-quadruplexes have been carried out in dilute solutions. However, the intracellular environment is highly crowded due to the presence of high concentrations of soluble and insoluble biomolecules.<sup>35–37</sup> Up to 40% of the volume of a living cell is filled with various biomolecules, leading to molecular crowding conditions.<sup>38,39</sup> It has been demonstrated that molecular crowding critically affects the G-quadruplex in a number of ways. For example, molecular crowding induces a conformational change in G-quadruplexes from antiparallel to parallel.<sup>40–45</sup> It has further been suggested that the hydration change induced by molecular crowding of cosolutes increases the stability of G-quadruplexes,<sup>40,46</sup> which critically affects telomerase activity.<sup>47</sup> Trent's group further identified that hydration is a major determinant of G-quadruplex stability and conformation.<sup>48</sup> The increased stability of the G-quadruplex by molecular crowding indicates that G-quadruplexes are a valuable target for structural-target drug design. Importantly, Phan's group recently proved by NMR that the different G-quadruplex conformations under dilute conditions can be converted to a propeller-type parallel conformation under molecular crowding conditions in the presence of  $K^+$ , which is totally consistent with biophysical results.<sup>40–45,49</sup> These results clearly suggest that biophysical and biochemical studies of longer telomeric G-rich strands can give significant insight into the structure and stability of the telomeric G-rich strand under such cell-mimicking conditions. To date, however, there have been no studies of long telomeric DNA under molecular crowding conditions.

In the present work, a series of telomeric G-rich DNA sequences of  $d(T_2AG_3)_n$ , where  $n$  indicates the number of telomeric repeats, and 4, 8, 12, 16, and 20 correspond to 1, 2, 3, 4, and 5 G-quadruplex units, respectively, were designed and synthesized. We studied the structure and thermodynamics of these G-rich sequences under dilute and molecular crowding conditions by using non-denaturing polyacrylamide gel electrophoresis (PAGE), circular dichroism (CD) spectroscopy, and thermal melting analysis followed by UV spectroscopy. The results showed that the G-rich sequences folded into intramolecular G-quadruplexes under molecular crowding conditions and that their topological characters depend on the cation species. CD data further implied that every G-quadruplex unit in G-rich sequences has the same conformation under each condition. Higher stability of G-quadruplexes in crowded solutions compared to dilute solution was observed; however, thermodynamic analysis showed that the effect of

molecular crowding on the thermodynamic stability of the structure was reduced for longer DNAs. A hydration study further demonstrated that the interior of a G-quadruplex unit is dehydrated, whereas the space surrounding the TTA linker between two units is more hydrated upon structure folding. These results allow us to propose that the linkers between G-quadruplex units are ordered structures but not random coils, which has an important influence on the stability of the entire structure of long telomeric DNAs.

## EXPERIMENTAL SECTION

**Materials.** Oligodeoxynucleotides used in this study were purchased from Hokkaido System Science Co., Ltd. (Hokkaido, Japan) after purification by high pressure liquid chromatography (HPLC). Single-strand concentrations of the DNA oligodeoxynucleotides were determined by measuring the absorbance at 260 nm and high temperature using a UV-1700 spectrometer (Shimadzu Co., Ltd., Kyoto, Japan) connected to a Shimadzu TMSPC-8 thermoprogrammer (Shimadzu Co., Ltd.). Single-strand extinction coefficients were calculated from mononucleotide and dinucleotide data using the nearest-neighbor approximation.<sup>50</sup> All chemical reagents were of reagent grade from Wako Pure Chemical Co., Ltd. (Osaka, Japan) and used without further purification.

**Nondenaturing PAGE.** Samples (1  $\mu$ L; 10  $\mu$ M) were separated by non-denaturing PAGE on 20% acrylamide (19:1 acrylamide/bisacrylamide) gels at 5 V  $cm^{-1}$  and 4  $^{\circ}C$ . A molecular crowding reagent, PEG 200 (poly(ethylene glycol) with an average molecular weight of 200), was not added to the polyacrylamide gel. Once a G-quadruplex has formed under dilute or molecular crowding conditions, the structure will take hours or more to undergo a conformational transition at low temperature. The PAGE experiments in this study were carried out at 4  $^{\circ}C$ ; therefore, the G-quadruplexes in the gel can be considered to have preserved the conformations formed in the respective buffer conditions. Gels were stained with GelStar nucleic acid gel stain (Cambrex, Baltimore, MD, U.S.) and imaged with FLS-5100 film (Fuji Film Co. Ltd., Tokyo, Japan). All measurements were carried out in 50 mM Tris-HCl buffer (pH 7.0). Before measurements, the samples were annealed by heating to 90  $^{\circ}C$  for 10 min, cooling to 4 at 0.5  $^{\circ}C min^{-1}$ , and incubation at 4  $^{\circ}C$  for 12–15 h.

**CD Spectroscopy.** The G-quadruplex structure has characteristic peaks in CD spectroscopy. Antiparallel G-quadruplexes show positive and negative peaks around 295 and 265 nm, respectively, whereas parallel G-quadruplex structures show positive and negative peaks around 260 and 240 nm, respectively.<sup>51</sup> Moreover, a hybrid-type G-quadruplex shows two positive peaks at 295 and 265 nm, and a negative peak at 240 nm.<sup>51</sup> CD spectra of DNA oligonucleotides were measured for 10  $\mu$ M DNA total strand concentration in a buffer containing 50 mM Tris-HCl (pH 7.0) and 100 mM NaCl or KCl at 0 wt % or 20 wt % PEG 200 using a J-820 spectropolarimeter (JASCO Co. Ltd., Hachioji, Japan) with a 0.1-cm path length quartz cell at 4  $^{\circ}C$ . The CD spectrum was obtained by taking the average of three scans made at 0.5 nm intervals from 200 to 350 nm. Before measurement, the DNA samples were heated at 90  $^{\circ}C$  for 10 min,

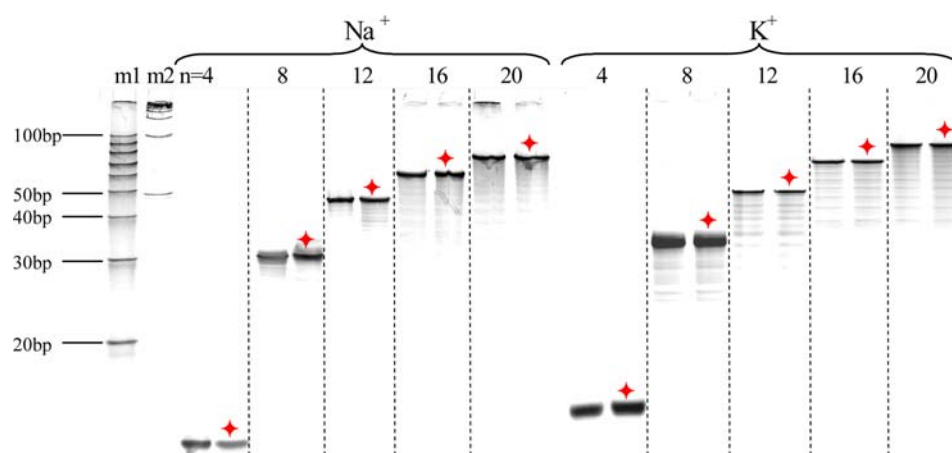


**Figure 2.** Nondenaturing 20% PAGE images of  $(T_2AG_3)_n$  ( $n = 4–20$ ) in the presence of 100 mM  $Na^+$  and 100 mM  $K^+$ , respectively, at 4 °C, pH 7.0. For each sequence, the sample loaded on the left is without 20% PEG 200, and the sample loaded on the right labeled with a red asterisk is with 20% PEG 200. Lane m1, 10-bp DNA standard; lane m2, 50-bp DNA standard.

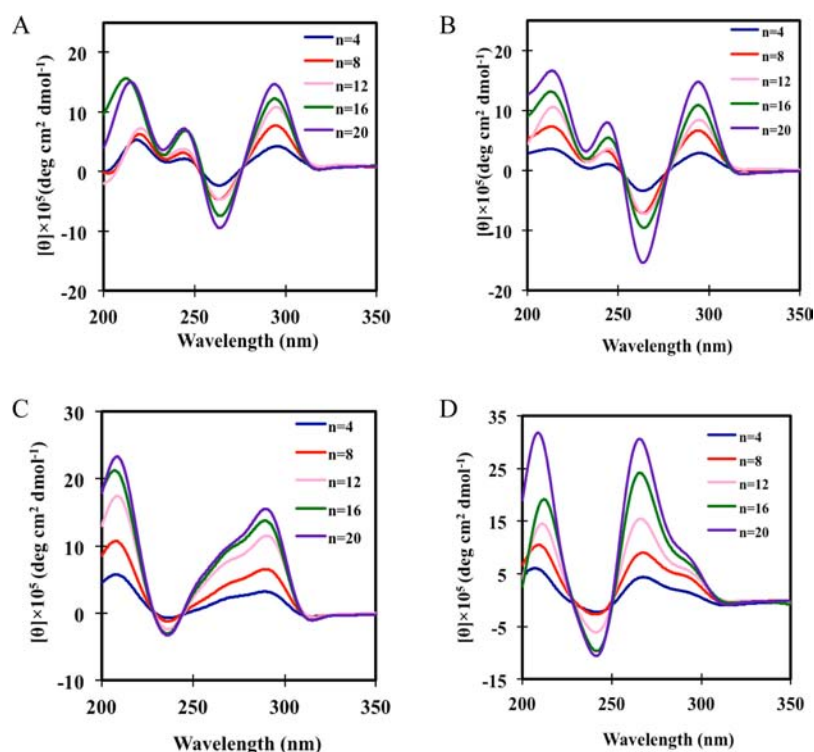


**Figure 3.** (A) CD spectra of  $(T_2AG_3)_n$  ( $n = 4–20$ ) measured at 4 °C in 50 mM Tris-HCl buffer (pH 7.0) containing 100 mM  $Na^+$ . (B) CD spectra of  $(T_2AG_3)_n$  ( $n = 4–20$ ) measured at 4 °C in 50 mM Tris-HCl buffer (pH 7.0) containing 100 mM  $Na^+$  and 20% PEG 200. (C) CD spectra of  $(T_2AG_3)_n$  ( $n = 4–20$ ) measured at 4 °C in 50 mM Tris-HCl buffer (pH 7.0) containing 100 mM  $K^+$ . (D) CD spectra of  $(T_2AG_3)_n$  ( $n = 4–20$ ) measured at 4 °C in 50 mM Tris-HCl buffer (pH 7.0) containing 100 mM  $K^+$  and 20% PEG 200. [ $n = 4$  (blue),  $n = 8$  (red),  $n = 12$  (pink),  $n = 16$  (green),  $n = 20$  (purple)].

gently cooled at 0.5 °C  $min^{-1}$ , and incubated at 4 °C for 12–15 h. The temperature of the cell holder was regulated by a PTC-348 temperature controller (JASCO), and the cuvette-holding chamber was flushed with a constant stream of dry  $N_2$  gas to avoid water condensation on the exterior of the cuvette.

**Thermodynamic Analysis.** UV melting curves of G-quadruplexes were measured at 295 nm in a buffer containing 50 mM Tris-HCl (pH 7.0) and 100 mM NaCl or KCl with various concentrations of PEG 200 using a UV-1700 spectrometer (Shimadzu Co., Ltd.). Before measurement, the DNA samples were heated at 90 °C for 5 min, gently cooled from 90 to 0 °C at 0.5 °C  $min^{-1}$ , and incubated at 4 °C overnight. The samples were then heated from 0 to 90 °C at 0.5 °C  $min^{-1}$ . The temperature of the cell holder was controlled by the

TMSPC-8 temperature controller (Shimadzu Co., Ltd.), and water condensation on the exterior of the cuvette in the low temperature range was avoided by flushing with a constant stream of dry  $N_2$  gas. In order to calculate thermodynamic parameters, including the melting temperature ( $T_m$ ), the enthalpy change ( $\Delta H^\circ$ ), the entropy change ( $\Delta S^\circ$ ), and the free energy change at 37 °C ( $\Delta G_{37}^\circ$ ) for intramolecular G-quadruplex formation, the melting curves were fit to the theoretical equation for an intramolecular association.<sup>52</sup>

**Water Activity Measurements.** The water activity was determined by the osmotic stressing method via vapor phase osmometry using a model 5520XR pressure osmometer (Wescor, Logan, Utah, U.S.) or by freezing point depression osmometry using a Typ Dig. L osmometer (KNAUER, Berlin, Germany), with the

assumption that the cosolutes do not directly interact with the DNA samples.<sup>53–55</sup>

## RESULTS AND DISCUSSION

**Structures of Long Human Telomeric DNAs under Dilute and Molecular Crowding Conditions.** We carried out non-denaturing PAGE and CD experiments to study the structures of long telomeric DNAs at 0 wt % and 20 wt % PEG 200 (poly(ethylene glycol) with an average molecular weight of 200) as dilute and molecular crowding conditions, respectively. Figure 2 shows the results of non-denaturing PAGE for  $(T_2AG_3)_n$  ( $n = 4–20$ ) in the presence of 100 mM  $Na^+$  or  $K^+$ . For each sequence, left and right lines are at 0 wt % PEG 200 and at 20% PEG 200 (labeled with a red star), respectively. The same migration for each DNA under the dilute and molecular crowding conditions was observed, indicating that the structures of the telomeric DNAs had very similar molecular weights and shapes. On the basis of NMR results,  $(T_2AG_3)_4$  folds into an intramolecular G-quadruplex with an antiparallel conformation in the presence of  $Na^+$ .<sup>30</sup> In addition, a dimer of  $(T_2AG_3)_4$  containing 48 bases should migrate slower than or similar to the 20-bp duplex of 40 bases. However, the band of  $(T_2AG_3)_4$  ran much faster than the 20-bp marker. These results show that  $(T_2AG_3)_4$  folds into an intramolecular G-quadruplex. In the presence of  $K^+$ ,  $(T_2AG_3)_4$  showed an almost identical migration pattern, again indicating an intramolecular structure. By comparing all the other sequences  $(T_2AG_3)_n$  ( $n = 8, 12, 16, 20$ ) with  $(T_2AG_3)_4$ , it appears that all of the DNAs fold into intramolecular G-quadruplexes under all conditions.

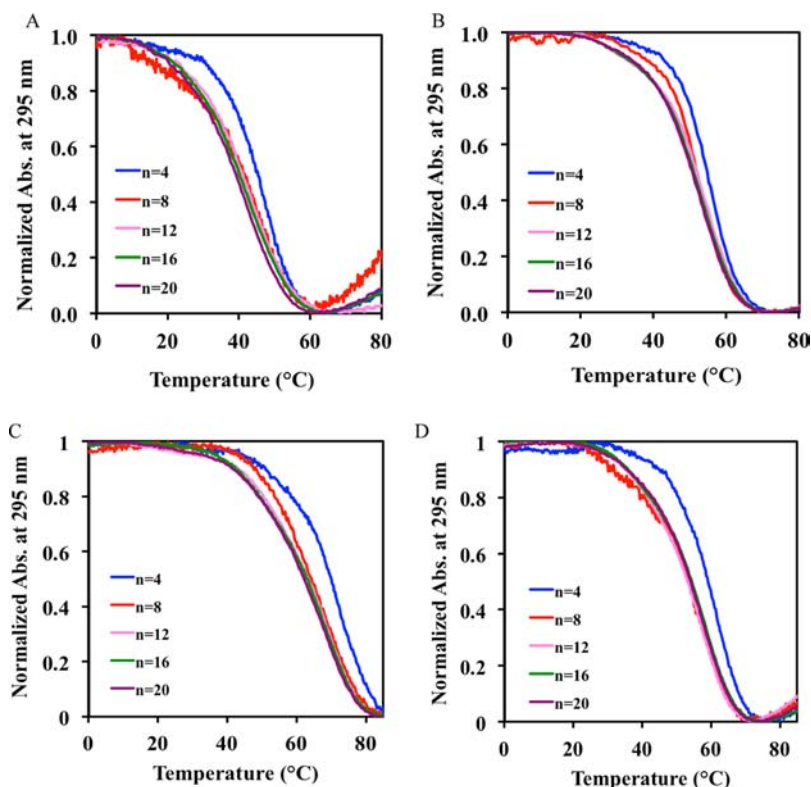
However, by comparing the migrations of  $(T_2AG_3)_4$  in the presence of  $Na^+$  and  $K^+$ , we found that the migrations in the presence of  $K^+$  were slightly slower than those in the presence of  $Na^+$ . This suggests that the structure of  $(T_2AG_3)_4$  in the presence of  $Na^+$  is more compact than that in the presence of  $K^+$ . In the presence of  $Na^+$ ,<sup>30</sup> the conformation of  $(T_2AG_3)_4$  is the basket-type antiparallel that has three diagonal loops, and in contrast,  $(T_2AG_3)_4$  folds into the (3 + 1) form of the G-quadruplex in the presence of  $K^+$  that has 1–3 propeller loops depending on the environment.<sup>31–33,49</sup> The loop type of a G-quadruplex conformation and its corresponding grooves may be the main reason for the differences in the compactness of G-quadruplexes. The other, longer DNAs ( $n = 8, 12, 16, 20$ ) showed the same difference in migration in the presence of  $Na^+$  and  $K^+$ , suggesting that the structure of the longer telomeric DNAs maintain the difference observed in the case of  $(T_2AG_3)_4$  depending on the coexisting cation,  $Na^+$  or  $K^+$ .

Figure 3A,B show the CD spectra of the  $(T_2AG_3)_n$  ( $n = 4–20$ ) under dilute and molecular crowding conditions in the presence of 100 mM  $Na^+$ . The CD spectrum of  $(T_2AG_3)_4$  showed a positive peak at 295 nm and a negative peak at 260 nm under the dilute condition (Figure 3A). This CD spectrum is typical for a G-quadruplex with an antiparallel conformation.<sup>51</sup> Although CD can hide the underlying complexity and polymorphism of G-quadruplex structures,<sup>50</sup> the folding of  $(T_2AG_3)_4$  into an antiparallel conformation in the presence of  $Na^+$  is consistent with a previous NMR result.<sup>30</sup> The longer sequences ( $n = 8, 12, 16, 20$ ) showed CD spectra with almost the same shape, suggesting that the G-quadruplexes were in an antiparallel conformation. Under the molecular crowding conditions,  $(T_2AG_3)_n$  ( $n = 4–20$ ) showed very similar CD spectra to those under the dilute conditions (Figure 3B). From these results, we concluded that the telomeric DNAs formed

antiparallel conformations under both conditions, supporting the non-denaturing PAGE results. These results are consistent with previous studies reporting that the G-quadruplex unit,  $(T_2AG_3)_4$ , maintains an antiparallel conformation even under molecular crowding conditions in the presence of  $Na^+$ .<sup>42,57</sup> Thus, we confirmed that long telomeric DNAs involving several G-quadruplex units also adopt the same conformation as isolated monomeric G-quadruplex units.

Figure 3C shows the CD spectra of  $(T_2AG_3)_n$  ( $n = 4–20$ ) under the dilute condition in the presence of 100 mM  $K^+$ . The CD spectrum of  $(T_2AG_3)_4$  had two positive peaks around 265 and 290 nm. Recently, G-quadruplex studies by NMR and CD spectrometry showed that the two positive peaks are a signature of the mixed (3 + 1) G-quadruplex conformation.<sup>18,19,32,57</sup> All of the other telomeric DNAs ( $n = 8, 12, 16, 20$ ) also had two similar positive peaks, indicating the formation of the mixed conformation. Thus, it is possible that the telomeric DNAs fold into a mixed conformation under dilute conditions in the presence of  $K^+$ . Figure 3D shows the CD spectra of  $(T_2AG_3)_n$  ( $n = 4–20$ ) under the molecular crowding condition in the presence of 100 mM  $K^+$ . Similar to the results under the dilute condition, the CD spectra had two positive peaks around 265 and 290 nm. It should be noted that the peak intensity around 265 nm became larger and the positive peak around 290 nm became smaller under molecular crowding conditions, indicating that molecular crowding induced a structural change in the presence of  $K^+$ . Recently, Tan and his co-workers showed a similar change in the CD spectra of  $G_3(T_2AG_3)_3$  induced by the addition of 40 wt % PEG 200.<sup>42</sup> They proposed that a parallel conformation was induced by molecular crowding conditions. Moreover, Phan's group demonstrated by NMR that human telomeric DNAs having four repeats folded to form mixed conformations under dilute conditions in the presence of  $K^+$ , whereas they folded into parallel conformations under molecular crowding conditions.<sup>49</sup> Combined with the results obtained here for long telomeric sequences and the recent biophysical and NMR studies for the short telomeric DNA sequences, it is obvious that molecular crowding induces a parallel conformation in the G-quadruplex units of long telomeric DNAs in the presence of  $K^+$ .

Notably, the CD spectra of  $(T_2AG_3)_n$  ( $n = 4–20$ ) have isodichroic points in each experimental condition (Figure 3). The isodichroic points in these CD spectra indicate that the structures of these telomeric DNAs generating the CD signal are the same with each other under each condition.<sup>58</sup> In addition, under the dilute and molecular crowding conditions in the presence of  $Na^+$ , the CD intensity at 293 nm has a linear relationship with the number of G-quadruplex units (Figures S1A and S1B of the Supporting Information, SI). The linear relationship was also observed in the presence of  $K^+$  (Figure S1C and S1D of the SI). The linear relationships between the CD intensity and the number of G-quadruplex units in each condition suggests that every G-quadruplex unit in a long telomeric DNA folds into the same conformation, e.g., the five G-quadruplex units in  $(T_2AG_3)_{20}$  form an antiparallel conformation if the G-quadruplex unit,  $(T_2AG_3)_4$ , forms the antiparallel conformation. Otherwise, the CD intensity of a long telomeric DNA, which should be the sum of CD intensities of each G-quadruplex unit, cannot be in proportion to the number of G-quadruplex units. Taking the CD spectra, the isodichroic points, and the linear relationship between the CD intensity and the number of G-quadruplex units together, the following can be concluded: (1) The structure of the G-quadruplex units



**Figure 4.** (A) Normalized thermal melting profiles recorded at 295 nm of  $(T_2AG_3)_n$  ( $n = 4-20$ ) in the presence of 100 mM  $Na^+$  without 20% PEG 200; (B) normalized thermal melting profiles recorded at 295 nm of  $(T_2AG_3)_n$  ( $n = 4-20$ ) in the presence of 100 mM  $Na^+$  with 20% PEG 200. (C) Normalized thermal melting profiles recorded at 295 nm of  $(T_2AG_3)_n$  ( $n = 4-20$ ) in the presence of 100 mM  $K^+$  without 20% PEG 200; and (D) normalized thermal melting profiles recorded at 295 nm of  $(T_2AG_3)_n$  ( $n = 4-20$ ) in the presence of 100 mM  $K^+$  with 20% PEG 200. All measurements were carried out in the 50 mM Tris-HCl buffer (pH 7.0) [ $n = 4$  (blue),  $n = 8$  (red),  $n = 12$  (pink),  $n = 16$  (green),  $n = 20$  (purple)].

in a longer telomeric DNA is the same as the isolated G-quadruplex unit,  $(T_2AG_3)_4$ . (2) The structure of the G-quadruplex units is the antiparallel conformation in the presence of  $Na^+$  under dilute and molecular crowding conditions. (3) In the presence of  $K^+$ , the structures of the G-quadruplex units under dilute and molecular crowding conditions are the (3 + 1) mixed and parallel conformations, respectively. Therefore, we infer that under molecular crowding conditions, the longer telomeric DNAs containing 2, 3, 4, and 5 G-quadruplex units maintain the beads-on-a-string structure that was proposed for dilute conditions.<sup>16</sup> These results further indicate that previous studies of G-quadruplexes under molecular crowding conditions are useful for structural characterization of longer G-rich DNAs, because each bead in the beads-on-a-string structure of such longer G-rich sequences is the same as a structural unit composed of four repeats under both molecular crowding and dilute conditions in the presence of  $Na^+$  or  $K^+$ .

**Thermodynamic Properties of Long Human Telomeric DNA Structures under Molecular Crowding Conditions.** We next investigated the thermodynamic properties of the G-quadruplexes of  $(T_2AG_3)_n$  ( $n = 4-20$ ) under the dilute and molecular crowding conditions in the presence of 100 mM  $Na^+$  and 100 mM  $K^+$ . In the case of  $(T_2AG_3)_4$ , both the normalized UV melting and annealing curves of  $(T_2AG_3)_4$  under the dilute and molecular crowding conditions in the presence of  $Na^+$  and  $K^+$  have a single sigmoidal shape without hysteresis between the annealing and melting curves (Figures S2A and S2B of the SI). These results indicate that the structure folding of  $(T_2AG_3)_4$  undergoes a two-state transition

between the single strand and the G-quadruplex, which is consistent with previous reports.<sup>59,60</sup> Thermodynamic parameters of  $(T_2AG_3)_4$  were evaluated by analyzing UV melting curves at 295 nm.<sup>61</sup> Figures S2C and S2D of the SI show the melting temperatures,  $T_m$ s, of  $(T_2AG_3)_4$  under the dilute and molecular crowding conditions in the presence of  $Na^+$  and  $K^+$ . Those  $T_m$  values were independent of DNA concentration. The independence of  $T_m$  values was also observed for the longer sequences (data not shown). These results showed the intramolecular structures of  $(T_2AG_3)_n$  ( $n = 4-20$ ), which are consistent with the results of nondenaturing PAGE (Figure 2).

Recently, Petracone et al. proposed that intermediate species exist during the G-quadruplex folding of  $(TTAGGG)_8TT$  and  $(TTAGGG)_{12}TT$ , and fitted the melting curve with a sequential model.<sup>25</sup> This new progression raised an important point: the melting curves of the telomeric DNA sequences having more than two G-quadruplex units could not be fitted with the two-state model to get meaningful thermal parameters. Generally, when the van't Hoff enthalpy ( $\Delta H^\circ_{vH}$ ) evaluated from the optical melting curve is equal to the calorimetric enthalpy ( $\Delta H^\circ_{cal}$ ), the transition can be considered to proceed in a two-state manner.<sup>59,62,63</sup> However, if  $\Delta H^\circ_{vH}$  is significantly smaller than  $\Delta H^\circ_{cal}$ , then the transition involves a population of intermediate states, and if  $\Delta H^\circ_{vH}$  is significantly larger than  $\Delta H^\circ_{cal}$ , an aggregation process is involved.<sup>59,62,63</sup> Saccà et al. reported that the comparison between  $\Delta H^\circ_{vH}$  ( $-45.0$  kcal/mol) and  $\Delta H^\circ_{cal}$  ( $-41.5$  kcal/mol) for the thermal denaturation of a G-quadruplex structure of a 22AG oligo,  $d[AG_3(T_2AG_3)_3]$ , including four repeats, gave a ratio of  $r$  ( $= \Delta H^\circ_{vH}/\Delta H^\circ_{cal}$ ) as 1.08. This value was concluded to validate

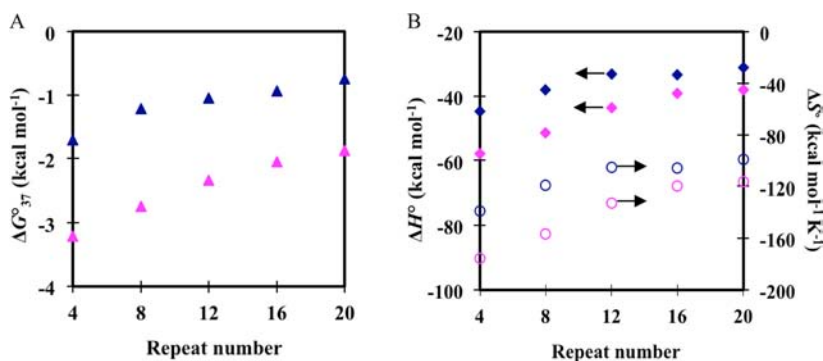


**Figure 5.** (A) The free energy ( $\Delta G_{37}^{\circ}$ ) values of the antiparallel G-quadruplexes of  $(T_2AG_3)_n$  ( $n = 4-20$ ) in the presence of 100 mM  $Na^+$ . (B) The enthalpy ( $\Delta H^{\circ}$ , diamond, left Y-axis) and entropy ( $\Delta S^{\circ}$ , circle, right Y-axis) values of the antiparallel G-quadruplexes of  $(T_2AG_3)_n$  ( $n = 4-20$ ) in the presence of 100 mM  $Na^+$ . Blue indicates dilute and pink indicates molecular crowding conditions.

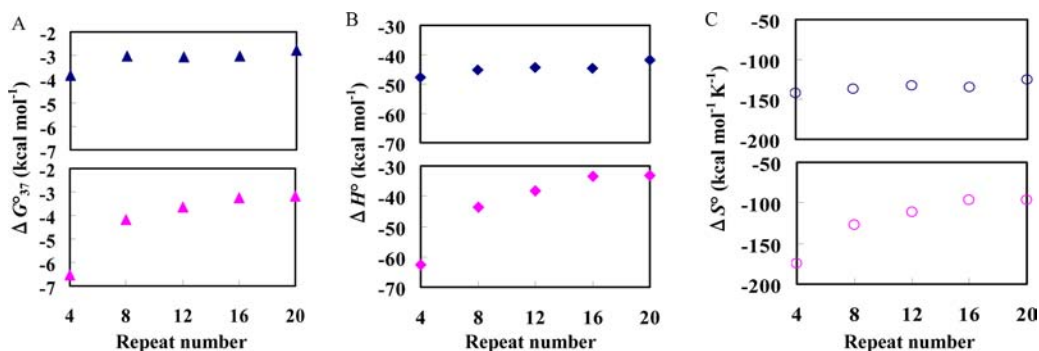


**Figure 6.** (A) The free energy ( $\Delta G_{37}^{\circ}$ ) values of the mixture type G-quadruplexes of  $(T_2AG_3)_n$  ( $n = 4-20$ ) in the presence of 100 mM  $K^+$ . (B) The enthalpy ( $\Delta H^{\circ}$ ) and values of the mixture type G-quadruplexes of  $(T_2AG_3)_n$  ( $n = 4-20$ ) in the presence of 100 mM  $K^+$ . (C) The entropy ( $\Delta S^{\circ}$ ) values of the mixture type G-quadruplexes of  $(T_2AG_3)_n$  ( $n = 4-20$ ) in the presence of 100 mM  $K^+$ . The top panel is the result for dilute conditions and the bottom panel is the result for molecular crowding conditions.

the two-state model in the thermal denaturation/renaturation process.<sup>60</sup> The  $r$  value of  $(T_2AG_3)_4$  can be estimated with  $\Delta H_{\text{vH}}^{\circ}$  ( $-47.8$  kcal/mol) obtained in the buffer containing 100 mM KCl and 50 mM Tris-HCl from the UV melting curve in this study, and  $\Delta H_{\text{cal}}^{\circ}$  ( $-41.5$  kcal/mol) of 22AG obtained in the buffer containing 100 mM KCl and 10 mM sodium cacodylate by Saccà et al.,<sup>60</sup> resulting in 1.2. From the value of  $\Delta H_{\text{cal}}^{\circ}$  ( $-54.5$  kcal/mol) of  $(T_2AG_3)_4$  obtained by Petraccone et al.,<sup>25</sup> the  $r$  value was evaluated to be 0.88. Both of the values are close to 1, suggesting that thermodynamic parameters with an assumption of a two-state transition are acceptable to show molecular crowding effects on the thermodynamics of G-quadruplexes. Furthermore, by comparing our data of  $\Delta H_{\text{vH}}^{\circ}$  for  $(T_2AG_3)_{n=4,8,12}$  with  $\Delta H_{\text{cal}}^{\circ}$  reported by Petraccone et al.,<sup>25</sup> it was found that the  $n$  values for  $(T_2AG_3)_{n=4,8,12}$  were 0.88, 0.74, and 0.97, respectively. Therefore, we consider that the values of  $\Delta H_{\text{vH}}^{\circ}$  for the longer sequences obtained from thermal melting curves allow us to evaluate the molecular crowding effects on the thermodynamics for the G-quadruplex formations, although the thermal denaturation process of some of these sequences involves an intermediate and/or is accompanied by a side reaction.<sup>25</sup>

The systemic thermodynamic data of  $(T_2AG_3)_n$  ( $n = 4-20$ ) were evaluated under dilute and crowding conditions in the presence of  $Na^+$  and  $K^+$ . Figure 4A,B shows UV melting curves of 5  $\mu\text{M}$   $(T_2AG_3)_n$  ( $n = 4-20$ ) under the dilute and crowding conditions in the presence of  $Na^+$ . From these melting curves with the two-state assumption, we evaluated the thermodynamic parameters of enthalpy change ( $\Delta H^{\circ}$ ), entropy change

( $\Delta S^{\circ}$ ), and free energy change at 37 °C ( $\Delta G_{37}^{\circ}$ ) for the G-quadruplex formation of  $(T_2AG_3)_n$  ( $n = 4-20$ ). The values of  $\Delta G_{37}^{\circ}$  under the dilute and molecular crowding conditions in the presence of  $Na^+$  showed that the G-quadruplex structures were stabilized by molecular crowding (Figure 5A). In addition, we found that the thermodynamic stability of the G-quadruplex decreased with the larger unit number. Moreover, the values of  $\Delta H^{\circ}$  and  $\Delta S^{\circ}$  under the same conditions (Figure 5B) showed the following: (1) Molecular crowding decreases  $\Delta H^{\circ}$  and  $\Delta S^{\circ}$  values. These results suggest that the stabilization of the G-quadruplexes of the telomeric DNA sequences is due to the favorable enthalpy change over the unfavorable entropy change. This is consistent with the results for short G-quadruplexes.<sup>46</sup> (2) The  $\Delta H^{\circ}$  and  $\Delta S^{\circ}$  values increase with the increment of the sequence length. Thus, the destabilization depending on the sequence length is enthalpically driven as reported previously.<sup>25,29</sup> Likewise, Figure 4B,C show the UV melting curves for 5  $\mu\text{M}$   $(T_2AG_3)_n$  ( $n = 4-20$ ) under the dilute and molecular crowding conditions in the presence of  $K^+$ . Figure 6 shows the thermodynamic parameters for G-quadruplexes of  $(T_2AG_3)_n$  ( $n = 4-20$ ) under the dilute (top panels) and molecular crowding (bottom panels) conditions. Note that based on the CD analysis, the structure of the telomeric DNA has a different conformation under the dilute and the molecular crowding conditions, the (3 + 1) and the parallel conformations, respectively, in the presence of  $K^+$ . Under the dilute condition, the values of  $\Delta G_{37}^{\circ}$ ,  $\Delta H^{\circ}$ , and  $\Delta S^{\circ}$  for the (3 + 1) G-quadruplex formations of  $(T_2AG_3)_n$  ( $n = 4-20$ ) were almost independent of the sequence length, except for  $(T_2AG_3)_4$ .

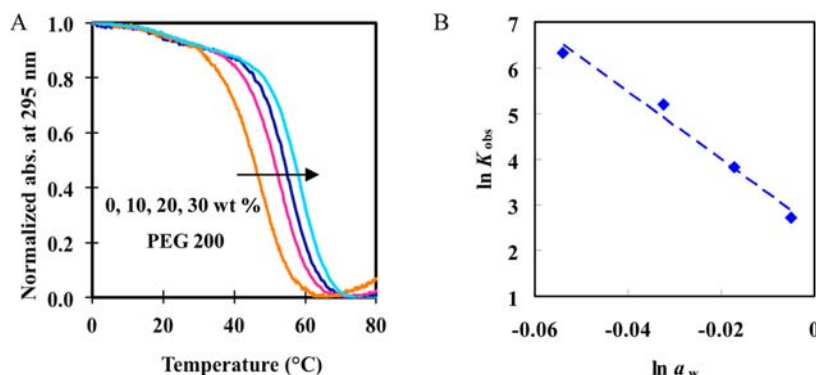


**Figure 7.** (A) Normalized UV melting curves for 5  $\mu\text{M}$   $(\text{T}_2\text{AG}_3)_4$  in the 50 mM Tris-HCl buffer (pH 7.0) with 100 mM  $\text{Na}^+$  containing 0 (orange), 10 (pink), 20 (blue), or 30 (light blue) wt% PEG 200. (B) Plot of  $\ln K_{\text{obs}}$  versus  $\ln a_w$  for the G-quadruplex formation of  $(\text{T}_2\text{AG}_3)_4$  in the 50 mM Tris-HCl buffer (pH 7.0) with 100 mM  $\text{Na}^+$  containing 0, 10, 20, or 30 wt % PEG 200.

However, under the molecular crowding condition, the parallel G-quadruplexes of  $(\text{T}_2\text{AG}_3)_n$  ( $n = 4-20$ ) showed an increasing trend of their  $\Delta G^\circ_{37}$ ,  $\Delta H^\circ$ , and  $\Delta S^\circ$  values following DNA length growth. The increment of thermodynamic parameters, however, becomes smaller for the longer DNA sequences. This is consistent with what we observed in the presence of  $\text{Na}^+$ . Therefore, although the characteristic thermodynamic parameters of  $(\text{T}_2\text{AG}_3)_n$  ( $n = 4-20$ ) are not entirely identical to each other due to the species of cation and the conformation of G-quadruplex, it is likely that the molecular crowding conditions generally have a greater effect on a shorter DNA.

These results demonstrate three important points. First, molecular crowding stabilizes the G-quadruplexes of these sequences. This stabilization effect of molecular crowding is totally consistent with its effect on the thermodynamics of G-quadruplexes of short telomeric DNA sequences.<sup>36,46,48</sup> Second, the  $\Delta G^\circ_{37}$  value increases with the length of the sequence, showing that the longer telomeric G-quadruplexes are less stable than the shorter ones. Third, and most importantly, the degree of the stabilization by molecular crowding,  $\Delta\Delta G^\circ_{37(\text{dilute})} = \Delta G^\circ_{37(\text{dilute})} - \Delta G^\circ_{37(\text{crowd})}$ , generally decreased with the increment of the sequence length. This indicates that the molecular crowding effect becomes smaller for the longer telomeric DNA sequences. The possible mechanism for these observations will be further discussed in the next section.

#### Hydration of Long Telomeric DNA G-Quadruplexes.

Since the hydration state is directly associated with the thermodynamic character of the G-quadruplex, we investigated the behavior of water molecules coordinating with long telomeric DNA G-quadruplexes to elucidate how molecular crowding differentially affects long and short telomeric DNA sequences.

Because all DNA sequences maintain the same G-quadruplex under dilute and molecular crowding conditions in the presence of  $\text{Na}^+$ , it is sufficient to study the hydration state of long telomeric DNA G-quadruplexes. It was previously demonstrated that water molecules are released upon G-quadruplex folding.<sup>40,46</sup> The number of water molecules taken up upon folding can be evaluated by the following equation:

$$\frac{d \ln K_{\text{obs}}}{d \ln a_w} = - \left[ \Delta n_w + \Delta n_{\text{CS}} \left( \frac{d \ln a_{\text{CS}}}{d \ln a_w} \right) + \Delta n_{\text{M}^+} \left( \frac{d \ln a_{\text{M}^+}}{d \ln a_w} \right) \right] \quad (1)$$

where  $K_{\text{obs}}$  is the observed equilibrium constant;  $a_w$ ,  $a_{\text{CS}}$ , and  $a_{\text{M}^+}$  are the activities of water, cosolute (PEG 200), and cation ( $\text{Na}^+$ ), respectively; and  $\Delta n_w$ ,  $\Delta n_{\text{CS}}$ , and  $\Delta n_{\text{M}^+}$  are the numbers of water, cosolute (PEG 200), and cation ( $\text{Na}^+$ ) molecules, respectively, released<sup>53-55</sup> upon formation of an antiparallel G-quadruplex.

Figure 7A shows normalized UV melting curves at 295 nm for the G-quadruplex of  $(\text{T}_2\text{AG}_3)_4$  with various concentrations of PEG 200. As the PEG 200 concentration was increased from 0 to 30 wt %, the  $T_m$  value of the G-quadruplex increased, which is the same tendency with various telomeric DNAs including four G-rich repeats.<sup>40,41,45,46,51</sup> From these melting curves, we further evaluated the  $K_{\text{obs}}$  values for the G-quadruplex formations. Figure 7B shows a plot of  $\ln K_{\text{obs}}$  at 37  $^\circ\text{C}$  for the G-quadruplex formation of  $(\text{T}_2\text{AG}_3)_4$  versus  $\ln a_w$ , which was determined by osmotic pressure measurements. The linear relationship between  $\ln K_{\text{obs}}$  and  $\ln a_w$  indicates that the slope is approximately equal to the number of water molecules taken up upon G-quadruplex formation.<sup>64</sup> The plots of  $\ln K_{\text{obs}}$  for G-quadruplex formation of  $(\text{T}_2\text{AG}_3)_n$  ( $n = 8-20$ ) versus  $\ln a_w$  are shown in Figure S3 of the SI. All of the plots had a negative slope, demonstrating release of water molecules (dehydration) upon G-quadruplex formation. The numbers of water molecules released upon folding are listed in Table 1. We found that the longer telomeric DNAs released slightly fewer water molecules upon G-quadruplex formation. The sequence of  $(\text{T}_2\text{AG}_3)_4$  folded into a G-quadruplex unit. Thus, it is notable that a total of 74 water molecules are released from one G-quadruplex unit. This number is comparable with the number

**Table 1.** Number of Water Molecules Released upon G-Quadruplex Structure Folding ( $\Delta n_w$ ) and the Coupling Free Energy ( $\Delta G^\circ_{\text{Coupling}}$ )<sup>a</sup> of  $(\text{T}_2\text{AG}_3)_n$  ( $n = 4-20$ )

telomeric repeat number ( $n$ )	$\Delta n_w$	$\Delta G^\circ_{\text{Coupling}}$ under dilute condition (kcal mol <sup>-1</sup> )	$\Delta G^\circ_{\text{Coupling}}$ under molecular crowding condition (kcal mol <sup>-1</sup> )
4	-73.8 $\pm$ 2.5		
8	-69.6 $\pm$ 7.2	+1.64	+4.68
12	-66.1 $\pm$ 4.9	+2.28	+8.67
16	-65.7 $\pm$ 3.3	+3.24	+13.1
20	-66.6 $\pm$ 3.4	+5.30	+16.7

<sup>a</sup> $\Delta G^\circ_{37(\text{Coupling})}$  was evaluated as the following equation:  $\Delta G^\circ_{37(\text{Coupling})} = \Delta G^\circ_{37(n)} \times n/4 - \Delta G^\circ_{37(n=4)} \times n/4$ , where  $n$  is the repeat number in the telomeric DNAs;  $\Delta G^\circ_{37(n)}$  is the free energy change of  $(\text{T}_2\text{AG}_3)_n$ ; and  $\Delta G^\circ_{37(n=4)}$  is the free energy change of  $(\text{T}_2\text{AG}_3)_4$ .

of water molecules released upon G-quadruplex formation as reported previously.<sup>46,65</sup> Likewise, the number of water molecules released through the folding of  $(T_2AG_3)_8$ , which includes two G-quadruplex units, is supposed to be about  $74 \times 2 = 148$ . However, the experimental value of released water molecules upon each unit formation of  $(T_2AG_3)_8$  is about 70. Since each G-quadruplex unit folds and unfolds individually, this number corresponds to the number of water molecules released from each unit in  $(T_2AG_3)_8$ . Thus, the total number of water molecules released from  $(T_2AG_3)_8$  composing two G-quadruplex units is  $70 \times 2 = 140$ , which is smaller than 148, the number that is as twice as  $(T_2AG_3)_4$ . This difference suggests that a part of the structure of  $(T_2AG_3)_8$  takes up water molecules upon folding. According to the beads-on-a-string structure of long G-rich telomeric DNA,<sup>16</sup> it is possible that the structure of the three-nucleotide TTA linker between two G-quadruplexes can affect the state of hydration. On the basis of this assumption, we can evaluate that the number of water molecules taken up by the structured linker between two G-quadruplexes is about 8–11, according to the number of released water molecules by  $(T_2AG_3)_n$  ( $n = 4–20$ ), demonstrating for the first time that a nonbase paired region of a DNA structure participates in controlling the hydration state of the entire structure. The hydration upon folding indicates that the TTA linker between two G-quadruplex units is not a random coil, but has a certain structure, which provides a scaffold for water coordination for the functional groups of the linker bases. In addition, it shows that the hydration states of the linkers in the structures of  $(T_2AG_3)_n$  ( $n = 8–20$ ) are similar to each other as the beads (the G-quadruplex units) in the beads-on-a-string are similar with each other. Notably, specific cation binding sites have been observed within the loops of G-quadruplex.<sup>67</sup> Phan et al. showed by NMR that  $K^+$  binds to the TTA loops in the human telomere G-quadruplex.<sup>68</sup> Moreover, Ida and Wu demonstrated  $Na^+$  binding to the TTTT loops of  $(G_4T_4T_4)$ .<sup>68</sup> They proposed that the coordination site of  $Na^+$  was the four O6 atoms of guanine bases, the O2 atom of a loop thymine, and a water molecule. These results indicate that the TTA linkers connecting the G-quadruplex units are potential cation binding sites, and that cation binding should accompany the uptake of water molecules. Consequently, although more structural determinations for the long telomeric DNAs by NMR or X-ray are required, these results lead us to conclude that the structure of long telomeric DNAs consists of G-quadruplexes and structured linkers, which release and take up water molecules, respectively, upon folding (Figure 8).

**The TTA Linker Affects the Hydration and Thermodynamics of the Beads-on-a-string Structure of Telomeric DNA Sequences.** What is the significance of the structured TTA linker with hydration upon folding? Previous studies have proposed a “beads-on-a-string” model as a possible structure of long G-rich telomeric DNA sequences, which generally contain ~200 bases as a single-stranded overhang. We previously proposed a simple beads-on-a-string structure, assuming that the beads (G-quadruplex units) independently folded and there was no interaction between contiguous beads.<sup>16</sup> A recent attempt was made using a combination of CD, sedimentation velocity, DSC, and molecular dynamics simulations to elucidate the detailed structure of long G-rich telomeric DNAs.<sup>25</sup> On the basis of the destabilization of dimer and trimer G-quadruplex units, that study demonstrated that each bead in the beads-on-a-string structure was not independent, but was thermodynamically

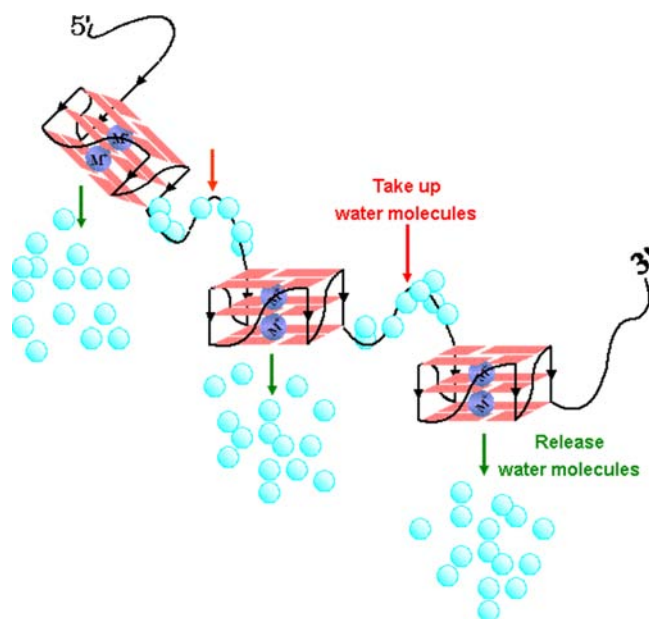


**Figure 8.** Scheme of hydration of the G-quadruplex structure of a long telomeric DNA. Light blue circles indicate water molecules and dark blue circles with  $M^+$  indicate cations.

cally unique and affects the neighboring beads. In order to quantify the interaction between the beads, the same authors introduced the coupling free energy ( $\Delta G^{\circ}_{\text{Coupling}}$ ), defined as the difference between the total free energy change of the folding of multiple G-quadruplex units, and the value obtained by multiplying the number of G-quadruplex units by the folding free energy change of a single G-quadruplex unit.<sup>25</sup> Here we express the definition of  $\Delta G^{\circ}_{\text{Coupling}}$  by the following equation:

$$\Delta G^{\circ}_{37(\text{Coupling})} = \Delta G^{\circ}_{37(n)} \times \frac{n}{4} - \Delta G^{\circ}_{37(n=4)} \times \frac{n}{4} \quad (2)$$

where  $n$  is the repeat number in the telomeric DNAs;  $\Delta G^{\circ}_{37(n)}$  is the free energy change of  $(T_2AG_3)_n$ ; and  $\Delta G^{\circ}_{37(n=4)}$  is the free energy change of  $(T_2AG_3)_4$ .

In the present study, under dilute conditions, the difference between three times the  $\Delta G^{\circ}_{37}$  of  $(T_2AG_3)_4$  ( $-3.84 \text{ kcal mol}^{-1}$ ) and three times the average  $\Delta G^{\circ}_{37}$  of each unit of  $(T_2AG_3)_{12}$  ( $-3.08 \text{ kcal mol}^{-1}$ ) was calculated as  $+2.28 \text{ kcal mol}^{-1}$  (Table 1). This positive value indicates an unfavorable interaction between the G-quadruplex units and is very similar with the  $\Delta G^{\circ}_{\text{Coupling}}$  reported previously,<sup>25</sup> although the origin for this  $\Delta G^{\circ}_{\text{Coupling}}$  had not been explained. In the same manner,  $\Delta G^{\circ}_{\text{Coupling}}$  for  $(T_2AG_3)_8$ ,  $(T_2AG_3)_{16}$ , and  $(T_2AG_3)_{20}$  was evaluated to be  $1.64 \text{ kcal mol}^{-1}$ ,  $+3.24 \text{ kcal mol}^{-1}$ , and  $+5.30 \text{ kcal mol}^{-1}$ , respectively, under the dilute condition. Moreover, the  $\Delta G^{\circ}_{\text{Coupling}}$  of  $(T_2AG_3)_8$ ,  $(T_2AG_3)_{12}$ ,  $(T_2AG_3)_{16}$ , and  $(T_2AG_3)_{20}$  was evaluated to be  $+4.68 \text{ kcal mol}^{-1}$ ,  $+8.67 \text{ kcal mol}^{-1}$ ,  $+13.1 \text{ kcal mol}^{-1}$ , and  $+16.7 \text{ kcal mol}^{-1}$ , respectively, under the molecular crowding condition. The  $\Delta G^{\circ}_{\text{Coupling}}$  value of the long telomeric DNAs under both conditions generally increases with the sequence length. This trend is also consistent with the previous report.<sup>25</sup> Interestingly, our data further showed that the coupling free energy became more unfavorable under the molecular crowding conditions, indicating that the role of the TTA linker is more significant under molecular crowding.

From this point of view, our results provide new insight into the interactions between G-quadruplex units under the

molecular crowding condition, generating the positive coupling free energy. The molecular crowding effects showed that the interior of the G-quadruplex unit is dehydrated upon folding, and the space surrounding the TTA linker between two G-quadruplex units is more hydrated, indicating the formation of an ordered structure of the linker region. Thus, it is considerable that the origin of the positive coupling energy is the ordered structure of the linker, which is more unfavorable under molecular crowding conditions where the activity and molar ratio of water molecules is decreased. Our results suggest for the first time a detailed structure of long telomeric DNA and its hydration microenvironment, which is significant not only for telomere biology, but also for rational drug design targeting telomeric DNA.

## CONCLUSIONS

We found that long telomeric DNAs folded into intramolecular G-quadruplexes in the presence of both  $\text{Na}^+$  and  $\text{K}^+$ . In  $\text{Na}^+$  solution, the G-quadruplex adopts an antiparallel conformation in both dilute and molecular crowding conditions. In the presence of  $\text{K}^+$ , however, molecular crowding induced a conformational change from the mixed to the parallel. These topological characters of the G-quadruplex structure formed by telomeric DNA depend on the cation species and crowding conditions, but do not depend on the length of telomeric DNA. Moreover, we demonstrated that every G-quadruplex unit in a long telomeric DNA adapted the same conformation. According to the thermal analysis, the G-quadruplexes in molecularly crowded solutions were obviously more stable than in dilute solutions, and the effect of molecular crowding on the stability of the structure was reduced for the longer telomeric DNAs. Finally, our hydration study revealed that upon structure folding, the interior of the G-quadruplex unit is dehydrated, whereas the space surrounding the TTA linker between two units is more hydrated. Based on that, a detailed beads-on-a-string structure formed by long telomeric DNAs consisting of G-quadruplex units with structured linkers between them is hereby proposed; this has an important influence on the stability of the entire structure of long telomeric DNAs. Our results are significant not only for understanding the behavior of telomeres in vivo and telomeric related critical cell cycle, but also for drug design targeting telomeres and related proteins.

## ASSOCIATED CONTENT

### Supporting Information

Plot of CD intensity versus repeat number of  $(\text{T}_2\text{AG}_3)_n$ , annealing and melting profiles of  $(\text{T}_2\text{AG}_3)_4$ , plot of  $\ln K_{\text{obs}}$  versus  $\ln a_w$  of  $(\text{T}_2\text{AG}_3)_{n=8-20}$ . These materials are available free of charge via the Internet at <http://pubs.acs.org>.

## AUTHOR INFORMATION

### Corresponding Author

miyoshi@center.konan-u.ac.jp, sugimoto@konan-u.ac.jp

### Notes

The authors declare no competing financial interest.

## ACKNOWLEDGMENTS

This work was supported in part by the Grants-in-Aid for Scientific Research, the Innovative Areas "Nanomedicine Molecular Science" (No. 2306), and the "MEXT-Supported Program for the Strategic Research Foundation at Private

Universities" (2009-2014) from the Ministry of Education, Culture, Sports, Science and Technology, Japan, and the Hirao Taro Foundation of the Konan University Association for Academic Research.

## REFERENCES

- (1) Phan, A. T.; Mergny, J. L. *Nucleic Acids Res.* **2002**, *30*, 4618.
- (2) Klobutcher, L. A.; Swanton, M. T.; Donini, P.; Prescott, D. M. *Proc. Natl. Acad. Sci. U.S.A.* **1981**, *78*, 3015.
- (3) Henderson, E. R.; Blackburn, E. H. *Mol. Cell. Biol.* **1989**, *9*, 345.
- (4) McElligott, R.; Wellinger, R. *J. EMBO J.* **1997**, *16*, 3705.
- (5) Hardin, C. C.; Henderson, E.; Watson, T.; Prosser, J. K. *Biochemistry* **1991**, *30*, 4460.
- (6) Hardin, C. C.; Watson, T.; Corregan, M.; Bailey, C. *Biochemistry* **1992**, *31*, 833.
- (7) Ross, W. S.; Hardin, C. C. *J. Am. Chem. Soc.* **1994**, *116*, 6070.
- (8) Miura, T.; Benevides, J. M.; Thomas, G. J., Jr. *J. Mol. Biol.* **1995**, *248*, 233.
- (9) Hud, N. V.; Smith, F. W.; Anet, F. A.; Feigon, J. *Biochemistry* **1996**, *35*, 15383.
- (10) Hardin, C. C.; Corregan, M. J.; Lieberman, D. V.; Brown, B. A. *Biochemistry* **1997**, *36*, 15428.
- (11) Fulton, A. B. *Cell* **1982**, *30*, 345.
- (12) Wright, W. E.; Valere, M. T.; Kenneth, E. H.; Stephen, D. L.; Jerry, W. S. *Genes Dev.* **1997**, *11*, 2801.
- (13) Azzalin, C. M.; Reichenbach, P.; Khoriant, L.; Giulotto, E.; Lingner, J. *Science* **2007**, *318*, 798.
- (14) Schoeftner, S.; Blasco, M. A. *Nat. Cell Biol.* **2008**, *10*, 228.
- (15) Luke, B.; Lingner, J. *EMBO J.* **2009**, *28*, 2503.
- (16) Yu, H.; Miyoshi, D.; Sugimoto, N. *J. Am. Chem. Soc.* **2006**, *128*, 15461.
- (17) Parkinson, G. N.; Lee, M. P.; Neidle, S. *Nature* **2002**, *417*, 876.
- (18) Xu, Y.; Noguchi, Y.; Sugiyama, H. *Bioorg. Med. Chem.* **2006**, *14*, 5584.
- (19) Ambrus, A.; Chen, D.; Dai, J. X.; Bialis, T.; Jones, R. A.; Yang, D. *Nucleic Acids Res.* **2006**, *34*, 2723.
- (20) Haider, S.; Parkinson, G. N.; Neidle, S. *Biophys. J.* **2008**, *95*, 296.
- (21) Xu, Y.; Ishizuka, T.; Kurabayashi, K.; Komiyama, M. *Angew. Chem., Int. Ed.* **2009**, *48*, 7833.
- (22) Petraccone, L.; Trent, J. O.; Chaires, J. B. *J. Am. Chem. Soc.* **2008**, *130*, 16530.
- (23) Bauer, L.; Tluczkova, K.; Tothova, P.; Viglasky, V. *Biochemistry* **2011**, *50*, 7484.
- (24) Wang, H.; Nora, G. J.; Ghodke, H.; Opreko, P. L. *J. Biol. Chem.* **2011**, *286*, 7479.
- (25) Petraccone, L.; Spink, C.; Trent, J. O.; Garbett, N. C.; Mekmaysy, C. S.; Giancola, C.; Chaires, J. B. *J. Am. Chem. Soc.* **2011**, *133*, 20951.
- (26) Chang, C. C.; Chien, C. W.; Lin, Y. H.; Kang, C. C.; Chang, T. C. *Nucleic Acids Res.* **2007**, *35*, 2846.
- (27) Vorliczková, M.; Chládková, J.; Kejnovská, I.; Fialová, M.; Kypr, J. *Nucleic Acids Res.* **2005**, *33*, 5851.
- (28) Amrane, S.; Adrian, M.; Heddi, B.; Serero, A.; Nicolas, A.; Mergny, J. L.; Phan, A. T. *J. Am. Chem. Soc.* **2012**, *134*, 5807.
- (29) Payet, L.; Huppert, J. L. *Biochemistry* **2012**, *51*, 3154.
- (30) Wang, Y.; Patel, D. J. *Structure* **1993**, *1*, 263.
- (31) Ambrus, A.; Chen, D.; Dai, J.; Bialis, T.; Jones, R. A.; Yang, D. *Nucleic Acids Res.* **2006**, *34*, 2723.
- (32) Luu, K. N.; Phan, A. T.; Kuryavyi, V.; Lacroix, L.; Patel, D. J. *J. Am. Chem. Soc.* **2006**, *128*, 9963.
- (33) Phan, A. T.; Luu, K. N.; Patel, D. J. *Nucleic Acids Res.* **2006**, *34*, 5715.
- (34) Lim, K. W.; Amrane, S.; Bouaziz, S.; Xu, W.; Mu, Y.; Patel, D. J.; Luu, K. N.; Phan, A. T. *J. Am. Chem. Soc.* **2009**, *131*, 4301.
- (35) Minton, A. P. *Mol. Cell. Biochem.* **1983**, *55*, 119.
- (36) Zimmerman, S. B.; Trach, S. O. *J. Mol. Biol.* **1991**, *222*, 599.
- (37) Ellis, R. J.; Minton, A. P. *Nature* **2003**, *425*, 27.
- (38) Ellis, R. J. *Trends Biochem. Sci.* **2001**, *26*, 597.

- (39) Thirumalai, D.; Klimov, D. K.; Lorimer, G. H. *Proc. Natl. Acad. Sci. U.S.A.* **2003**, *100*, 11195.
- (40) Miyoshi, D.; Nakao, A.; Sugimoto, N. *Biochemistry* **2002**, *41*, 15017.
- (41) Zheng, K.; Chen, Z.; Hao, Y.; Tan, Z. *Nucleic Acids Res.* **2009**, *38*, 327.
- (42) Xue, Y.; Kan, Z.; Wang, Q.; Yao, Y.; Lui, J.; Hao, Y.; Tan, Z. *J. Am. Chem. Soc.* **2007**, *129*, 11185.
- (43) Vorlickova, M.; Bednarova, K.; Kypr, J. *Biopolymers* **2006**, *82*, 253.
- (44) Zhou, J.; Wei, C.; Jia, G.; Wang, X.; Feng, Z.; Li, C. *Chem. Commun.* **2010**, *46*, 1700.
- (45) Zhou, J.; Wei, C.; Jia, G.; Wang, X.; Tang, Q.; Feng, Z.; Li, C. *Biophys. Chem.* **2008**, *136*, 124.
- (46) Miyoshi, D.; Karimata, H.; Sugimoto, N. *J. Am. Chem. Soc.* **2006**, *128*, 7957.
- (47) Yu, H.; Zhang, D.; Gu, X.; Miyoshi, D.; Sugimoto, N. *Angew. Chem., Int. Ed.* **2008**, *47*, 9034.
- (48) Miller, M. C.; Buscaglia, R.; Chaires, J. B.; Lane, A. N.; Trent, J. *O. J. Am. Chem. Soc.* **2010**, *132*, 17105.
- (49) Heddi, B.; Phan, A. T. *J. Am. Chem. Soc.* **2011**, *133*, 9824.
- (50) Richard, E. G. *Handbook of Biochemistry and Molecular Biology*; CRC Press: Cleveland, OH, 1975.
- (51) Miyoshi, D.; Matsumura, S.; Nakano, S.; Sugimoto, N. *J. Am. Chem. Soc.* **2004**, *126*, 165.
- (52) Marky, L. A.; Breslauer, K. J. *Biopolymers* **1987**, *26*, 1601.
- (53) Nakano, S.; Karimata, H.; Ohmichi, T.; Kawakami, J.; Sugimoto, N. *J. Am. Chem. Soc.* **2004**, *126*, 14330.
- (54) Goobes, R.; Kahana, N.; Cohen, O.; Minsky, A. *Biochemistry* **2003**, *42*, 2431.
- (55) Rozners, E.; Moulder, J. *Nucleic Acid Res.* **2004**, *32*, 248.
- (56) Dailey, M. M.; Miller, M. C.; Bates, P. J.; Lane, A. N.; Trent, J. *O. Nucleic Acids Res.* **2010**, *38*, 4877.
- (57) Miyoshi, D.; Karimata, H.; Sugimoto, N. *Angew. Chem., Int. Ed.* **2005**, *117*, 3806.
- (58) Surovaya, A. N.; Grokhovsky, S. L.; Burckhardt, G.; Fritzsche, H.; Zimmer, Ch.; Gursky, G. V. *Mol. Biol.* **2002**, *36*, 726.
- (59) Marky, L. A.; Breslauer, K. J. *Biopolymers* **1987**, *26*, 1601.
- (60) Saccà, B.; Lacroix, L.; Mergny, J. L. *Nucleic Acids Res.* **2005**, *33*, 1182.
- (61) Mergny, J. L.; Phan, A. T.; Lacroix, L. *FEBS Lett.* **1998**, *435*, 74.
- (62) Sturtevant, J. M. *Annu. Rev. Phys. Chem.* **1987**, *38*, 463.
- (63) Spink, C. H. *Methods in Cell Biol.* **2008**, *84*, 115.
- (64) Vasilevskaya, V. V.; Khokhlov, A. R.; Matsuzawa, Y.; Yoshikawa, K. *Chem. J. Phys.* **1995**, *102*, 6595.
- (65) Gu, X.; Nakano, S.; Sugimoto, N. *Chem. Commun.* **2007**, *14*, 2750.
- (66) Hud, N. V.; Plavc, J. The Role of Cations in Determining Quadruplex Structure and Stability. In *Quadruplex Nucleic Acids*; Neidle, S., Balasubramanian, S., Eds.; Royal Society of Chemistry: Cambridge, U.K.; 2006, pp 100–130.
- (67) Phan, A. P.; Kuryavyi, V.; Luu, K. N.; Patel, D. J. *Nucleic Acids Res.* **2007**, *35*, 6517.
- (68) Ida, R.; Wu, G. J. *J. Am. Chem. Soc.* **2008**, *130*, 3590.